



HAL
open science

Barium Borosilicate Sealing Glasses Synthesized by a Sol-Gel Process: Chemical Interactions with a Stainless Steel and Gas-Tightness of a SOFC

Jean Puig, Florence Ansart, Pascal Lenormand, Nicolas Bailly, Samuel Georges, Julian Dailly

► **To cite this version:**

Jean Puig, Florence Ansart, Pascal Lenormand, Nicolas Bailly, Samuel Georges, et al.. Barium Borosilicate Sealing Glasses Synthesized by a Sol-Gel Process: Chemical Interactions with a Stainless Steel and Gas-Tightness of a SOFC. *Fuel Cells*, 2014, 14 (6), pp.1014-1021. 10.1002/fuce.201300289 . hal-01999471

HAL Id: hal-01999471

<https://hal.science/hal-01999471>

Submitted on 30 Jan 2019

HAL is a multi-disciplinary open access archive for the deposit and dissemination of scientific research documents, whether they are published or not. The documents may come from teaching and research institutions in France or abroad, or from public or private research centers.

L'archive ouverte pluridisciplinaire **HAL**, est destinée au dépôt et à la diffusion de documents scientifiques de niveau recherche, publiés ou non, émanant des établissements d'enseignement et de recherche français ou étrangers, des laboratoires publics ou privés.






Open Archive Toulouse Archive Ouverte (OATAO)

OATAO is an open access repository that collects the work of Toulouse researchers and makes it freely available over the web where possible

This is an author's version published in: <http://oatao.univ-toulouse.fr/21720>

Official URL: <https://doi.org/10.1002/fuce.201300289>

To cite this version:

Puig, Jean  and Ansart, Florence  and Lenormand, Pascal  and Bailly, Nicolas and Georges, Samuel and Dailly, Julian *Barium Borosilicate Sealing Glasses Synthesized by a Sol-Gel Process: Chemical Interactions with a Stainless Steel and Gas-Tightness of a SOFC*. (2014) *Fuel Cells*, 14 (6). 1014-1021. ISSN 1615-6846

Any correspondence concerning this service should be sent to the repository administrator: tech-oatao@listes-diff.inp-toulouse.fr

Barium Borosilicate Sealing Glasses Synthesized by a Sol–Gel Process: Chemical Interactions with a Stainless Steel and Gas-Tightness of a SOFC

J. Puig¹*, F. Ansart¹, P. Lenormand¹, N. Bailly², S. Georges², J. Dailly³

¹ CIRIMAT, Université Paul Sabatier, 118 route de Narbonne, 31062 Toulouse, France

² LEPMI, Université de Grenoble, 1130 rue de la Piscine, 38402 St Martin d'Hères, France

³ EIFER, Universität Karlsruhe - Emmy Noether Strasse 11, 76131 Karlsruhe, Germany

Abstract

Several glasses synthesized by sol–gel route and based on the $\text{BaO–B}_2\text{O}_3\text{–X–Al}_2\text{O}_3\text{–SiO}_2$ ($\text{X} = \text{CaO}, \text{MgO}$) glass system have been investigated to evaluate their applicability as sealant for solid oxide fuel cell (SOFC). Chemical interactions with K41X stainless steel and hydrogen-tightness of these materials were evaluated after operations at high temperatures over 1,000 h in air atmosphere. Formation of a new phase at the steel–glass interface and formation of porosity in the glass were observed and determined as critical problems over mid-term

operations. The role of MgO is important to obtain a gas-tight sealing. Application of the glass paste without binder addition was performed in order to avoid possible residual porosity related problems. The best glass was finally used as sealant between anodic and cathodic compartments in complete SOFCs operated at 760 and at 800 °C. Open circuit voltages and power densities of the cells were recorded during the first hours of operation.

Keywords: Durability, Electrical performance, Glass-sealant, Permeability, SOFC, Sol-gel

1 Introduction

Planar solid oxide fuel cell (SOFC) systems allow a direct conversion of chemical energy of a fuel into electrical energy. The high energy conversion efficiency and the low rate of emissions of these systems are the main reasons of their attractiveness. Most applications for power generation either stationary or mobile will be concerned by this technology [1]. One of the current challenges is the development of efficient glass–ceramic sealants to separate cathodic and anodic chambers in order to make a serial repeat unit (SRU), also called stack. Among the most promising materials, glass–ceramic sealants have been extensively studied for this application because of their good mechanical and electrical insulation properties and the possibility to use a wide range of chemical compositions to control some physicochemical properties such as viscosity, coefficient of thermal expansion, and glass transition temperature [2–4].

Barium–calcium aluminosilicate glass–ceramics (BCAS) are quite promising and have been developed to identify the respective contributions and influences of addition elements

[3–10]. These compositions result in partially crystallized materials with a relatively large glassy phase volume. Barium silicate crystals are formed, while other phases can be promoted or inhibited as a function of additive elements. This kind of glass crystallizes at lower temperature as compared to those based on other alkaline cations ($\text{Ca}^{2+}, \text{Mg}^{2+} \dots$) or to barium aluminosilicate glasses (BAS) [5]. The addition of B_2O_3 produces an expected decrease of the viscosity and a delay in the crystallization process. These phenomena lead to a greater wettability of the glasses on the steel, but B_2O_3 content must be quite low because of the formation of volatile compounds at high temperatures [6]. At a first glance, small additions of CaO , MgO , Y_2O_3 , La_2O_3 , and ZrO_2 seemed to have little impact on the thermomechanical properties of glass–ceramics [6]. Nonetheless, with an ageing of 200 h at 900 °C, devitrification of glass–ceramics are more advanced and different crystal phases appear in glass bulk. Some crystals cause a decrease of

[*] Corresponding author, jean.puig@cea.fr

the glass–ceramics CTEs, which can lead to a mismatch with the other cell components CTEs [7]. On the contrary, barium silicate crystal phases like BaSiO₃ (needle shaped) have high CTE (9.10⁻⁶–13.10⁻⁶ K⁻¹) [2]. Celsian phase, with a very low CTE, could be formed in barium silicate glass containing CaO or MgO [8]. An Al₂O₃ content inferior or equal to 5 mol.% improves the wetting behavior of a BBAS glass on YSZ and increases the stability of glass toward devitrification [9]. No chemical reactions have been observed at the interface BBAS glass-YSZ electrolyte [10]. However, barium silicate glasses showed a high reactivity at the steel–glass interface with the formation of an unsuitable phase BaCrO₄ with a high CTE using different steel chemical compositions (AISI446, Nicrofer6025HT and SS410) [11–15]. Iron oxide rich nodules have already been observed at the triple point air–glass–steel using CROFER22APU as interconnect material [16–18]. These nodules could rise to local short-circuiting effects, which probably results in stack failure.

Gas-tightness problems using these materials could appear for different reasons:

1. High porosity of the sealant after the sealing procedure because of a crystallization phenomenon beginning before the end of the maximum densification of the material.
2. Evolution of the CTE of the glass, which becomes very far from the CTE of the other cells components, could lead to cracks inside or at the interface between the two components.
3. Formation of a new chemical phase at an interface between two cells components. If this new phase has a very high CTE (like BaCrO₄ at the steel–glass interface) or a very low CTE, it could lead to cracks between components.
4. Formation of porosity in the glass during the cell working at high temperature. For instance, alloy elements can diffuse into the glass and react with the glass components or its impurities to form a gas phase. This gas, which could be dihydrogen, is trapped into the material, giving rise to pores [14].

Four thermally stable BBXAS glasses have been developed in a previous work [19]. The route we used in such a study is the sol–gel route because this soft chemistry process allows to decrease the processing temperatures of the glasses. We have lead tests in parallel on direct oxide mixture batch, and the characteristic temperatures were typically 1,150–1,300 °C compared to 1,400–1,550 °C for the same duration for, respectively, sol–gel route and solid–solid process. BaO content has been

fixed to 35 mol.% according to previous results showing that CTE of barium aluminosilicate material was suitable with that percentage [20]. Al₂O₃ content was determined at values lower than 5 mol.% considering Sun et al. study [9].

T_g of the as formed glasses was between 596 and 626 °C and CTE was close to 12–14 × 10⁻⁶ K⁻¹ [19]. These low T_g were due to a better homogeneity between cationic precursors by sol–gel inducing a more important reactivity of materials. The sealing temperature of these glasses was determined at 880 °C (duration of 10 h). Glasses exhibit thermal stability and good chemical compatibility with steel K41X over 100 h at 800 °C under air. Furthermore, crystalline phases of sealants were the same after the sealing operation and after the ageing treatment at high temperature. So, CTE were supposed to be stable over longer thermal treatments. Measurements of electrical resistivities after the sealing operation indicated that the four materials were suitable.

In this study, the thermal stability in air of the four glasses was investigated over 1,000 h at different temperatures. Hydrogen-tightness of steel–glass–steel assemblies and chemical reactions at the steel–glass interfaces were analyzed in order to evaluate the suitability of sealants over mid-term heat treatments. An assembly without binder has been elaborated and characterized with the most adequate sealant (relative to physico-chemical properties and to hydrogen-tightness tests) to reduce the amount of organic compounds in the shaping process.

Two cells were sealed with that glass paste and electrical tests were performed to confirm that the chosen material had appropriate sealing properties under SOFC working conditions.

2 Experimental

2.1 Synthesis of Glass–Ceramics by Sol–Gel Route

Four glass–ceramics were synthesized optimizing a sol–gel alkoxide route described in previous studies [19,20] and followed by a thermal treatment at 1,300 °C. Different parameters such as the alkoxide/solvent ratio, the duration between each step, and the $W = [H_2O]/[TEOS]$ and $R = [CH_3COOH]/[TEOS]$ ratios were optimized in order to obtain homogeneous gels. Amorphous BBXAS glasses (chemical compositions BaO–B₂O₃–X = MgO, CaO–Al₂O₃–SiO₂ in Table 1) were obtained after glass-processing at 1,300 °C [19].

Glasses were ground to obtain fine grains in order to perform thermal analyses. Grain sizes were determined by a laser

Table 1 Chemical compositions of glasses checked by ICP-AES.

Glasses	Chemical compositions by ICP-AES (mol.%)						Synthesis parameters	
	BaO	Al ₂ O ₃	B ₂ O ₃	MgO	CaO	SiO ₂	W	R
C1	39.1	2.7	9.8	0	10.5	38	70	2
C2	38.2	3.1	9.5	0	15.3	33.8	70	2
CM1	36.9	3	9.4	5.5	10.5	34.7	70	2.5
CM2	36.7	2.8	9.6	10.4	10.7	29.9	70	2.5

Table 2 Chemical composition of steel K41X.

K41X	Fe	Cr	Si	Nb	Mn	Ni	Ti	Cu	Others
Weight%	80.5	17.83	0.53	0.46	0.27	0.16	0.15	0.05	0.05

Table 3 Components of LEPMI cells used to perform electrical tests.

Anode (thickness)	Electrolyte (thickness)	Cathode (thickness)	Active area of the cathode
NiO–YSZ 1 mm	8YSZ 10 μm	LSM ~50 μm	0.79 cm ²

diffraction method, using a Beckman coulter LS Particle Size Analyzer (LMTG laboratory, Toulouse). All the powders were polydisperse with a median grain size (d_{50}) in volume in the range 16.3–19.3 μm. The grain size was smaller than 70 μm, which was suitable to seal SOFC components.

2.2 Preparation and Characterization of Steel–Glass–Steel Assemblies

In order to investigate the adhesion properties, sandwiched samples of two 1.5 mm thick plates of ferritic steel K41X of 50 mm × 50 mm (chemical composition in Table 2) were sealed with the glasses. One of the steel squares has a drill hole of 10 mm in the middle, which allows to perform the hydrogen gas-tightness test. The standard joining sample setting (application of the glass on steel plates, joining procedure) was established earlier by Gross et al. [21] and was used in a previous work [19]. Joining procedure was determined at 850 °C during 2 h under air atmosphere. Constant heating and cooling rate of 2 K min⁻¹ was used for all the joining experiments. Ageing processes in air atmosphere were performed in order to evaluate the evolution of the sealant in operating temperature (700 and 800 °C) after 1,000 h (mid-term tests). A joining test without binder was performed. Ethylcellulose and terpineol were substituted by water. An ageing test of 1,000 h in air was carried out on this assembly.

Hydrogen-tightness tests were performed on steel–glass–steel assemblies at room temperature under atmospheric pressure using an EX METER II detector of the brand MSA AUER (certified by EN50054 norm). A constant flux of ~4 L h⁻¹ was injected in assemblies. The hydrogen detection at the output of the device was regularly calibrated with a zirconia pellet (gas-tight reference). Considering the display accuracy of the detector (±2% between lower explosive limit and 100 vol.% of hydrogen), assemblies were considered gas-tight when the ratio of the measured flux on assemblies to the measured flux on zirconia reference at the device output was inferior to ±2 vol.%. The samples cross-sections were analyzed by scanning electron microscopy (JEOL JE6510LV model), coupled with energy dispersive X-ray detector (EDX). Microstructure analysis was used to determine the size and morphology of the crystals as well as to investigate potential chemical reactions at the glass–ceramics and steel interface in the samples during sealing and ageing procedure.

2.3 Electrochemical Tests on SOFCs Sealed with the Optimized Glass

Electrochemical tests were carried out on circular fuel cells obtained from Forschungszentrum Jülich as commercial NiO–YSZ/YSZ substrates with a graded LSM/YSZ–LSM cathode deposited at the LEPMI by a screen printing technique. These cells were sealed with the glass selected as the best compromise after the first experiments. The equipment and the procedure used to perform these tests have already been described in previous studies [22,23]. The cells were contacted using gold grids and gas diffusers applied on both electrodes with a controlled and reproducible pressure. Main characteristics of the cells components are presented in Table 3. The cells were sealed to an alumina ring using the glass paste (Figure 1). A circular gold wire ($\varnothing = 50$ mm) was used as a gasket to seal the alumina ring to the cathodic and anodic tubes.

The measurement of the open circuit voltage (OCV) of cells is directly correlated to the sealant quality by the Nernst equation:

$$\Delta E = \frac{RT}{4F} \ln \frac{P_{O_2,c}}{P_{O_2,an}} \quad (1)$$

where, R is the ideal gas constant, T is the absolute temperature, F the Faraday constant and $P_{O_2,c}$ and $P_{O_2,an}$ the oxygen partial pressure in the cathodic and anodic compartments, respectively.

The more the OCV was close to the theoretical value (1.13 V at 800 °C), the more the sealant was considered gas-tight. When the OCV was superior to 1.1 V, the sealant was considered gas-tight enough.

Polarization curves were recorded before and after a constant polarization at 0.5 V to evaluate the electrical performances of the cells. The power density (mW cm²) of cells was calculated from obtained data. Solartron electrochemical interface SI1287 coupled with a frequency response analyzer SI1250 were used for electrical and electrochemical characterization.

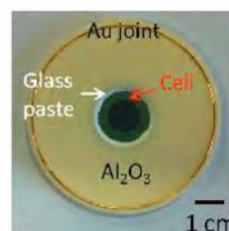


Fig. 1 Photograph of a cell sealed with the most suitable glass (of this study) to an alumina ring before sealing operation.

3 Results

3.1 Ageing Test of 1,000 h at 700°C

The photograph presented in Figure 2a present glasses paste deposits on 5 cm² steel square substrates before joining experiment. After a sealing treatment of the steel–glass–steel sandwiches at 850 °C during 2 h, followed by an ageing operation of 1,000 h at 700 °C in air, steel surfaces of assemblies were oxidized (Figure 2b). Nevertheless, a good adhesion was obtained on each sample.

The ratios of the hydrogen flux measured on steel–glass–steel assemblies to the hydrogen flux measured on zirconia reference at the output of the device of tightness tests (performed at room temperature after several ageing operations) are presented in Table 4. For all the assemblies, hydrogen fluxes were close to the hydrogen flux for zirconia reference. Indeed, relatives deviations were inferior to 2%, which was the accuracy for these tests. Therefore, all assemblies were considered gas-tight.

The SEM micrographs of Figure 3 demonstrate a good adhesion of the four glasses to the steel substrate. Some pores with a diameter of 20–40 μm were only observed in glasses C1 and C2. Pore diameters in the other glasses were inferior to 20 μm. Crystals with different compositions and morphologies were observed in the glasses. EDX measurements revealed the presence of barium–calcium silicate crystals in the gray areas. Barium silicates crystals (white areas) are also present in C1, C2, and CM1 glasses. These crystals have a more acicular shape in CM1 glass (1–3 μm wide and 10–20 μm in length). It is possible that the addition of MgO has promoted the formation and growth of these crystals as it had been already described in a previous study [17]. Small crystals (height ≤1 μm) are homogeneously dispersed in the CM2 glass. These crystals are composed of magnesium and silicon and were attributed to MgSiO₃ phase in a last work [19].

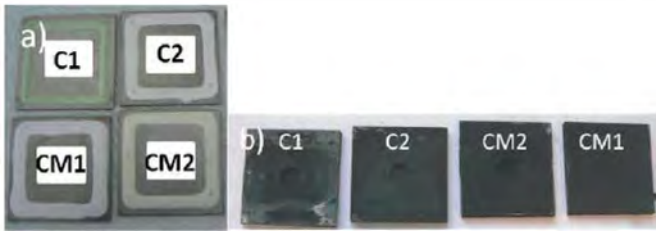


Fig. 2 Photographs of (a) glasses paste on steel plates, (b) steel–glass–steel sandwiches after a sealing operation at 850 °C during 2 h followed by a heat treatment at 700 °C of 1,000 h under air atmosphere.

Table 4 Results of hydrogen-tightness tests on steel–glass–steel assemblies at ambient temperature after different ageing operations at 700 °C (until 1,000 h) under air atmosphere (in vol.% of the measured flux on zirconia reference).

Samples	H ₂ out <i>t</i> = 0 h (vol.%)	H ₂ out <i>t</i> = 250 h (vol.%)	H ₂ out <i>t</i> = 500 h (vol.%)	H ₂ out <i>t</i> = 750 h (vol.%)	H ₂ out <i>t</i> = 1,000 h (vol.%)	Comments
C1	100	100	98.3	99.8	100.3	Gas-tight
C2	100	100	98	99.5	99.7	Gas-tight
CM1	100	100	98.3	99.5	100	Gas-tight
CM2	100	99.2	100	/	101.1	Gas-tight

3.2 Ageing Test of 1,000 h at 800°C

Sandwiched samples as described above (Section 2.2) were annealed at 800 °C for 1,000 h in air without thermal cycling. Heat treatments at higher temperature generally increase the chemical reactivity between glasses and steel.

Hydrogen-tightness measurements after this ageing operation showed that glasses C1 and C2 were not suitable to seal such assemblies because the ratio flux measured on assemblies/flux measured on reference was too low (see Table 5). CM1 glass did not provide a perfect sealing (relative deviation from zirconia reference at the device output is slightly superior to 2%) but the use of CM2 glass was satisfactory.

Observations of steel–glass interfaces performed after heat treatment (Figure 4) showed good adhesion between glasses and steel. No reaction was observed between C1, CM1, and CM2 glasses and steel K41X. On the other hand, a new phase

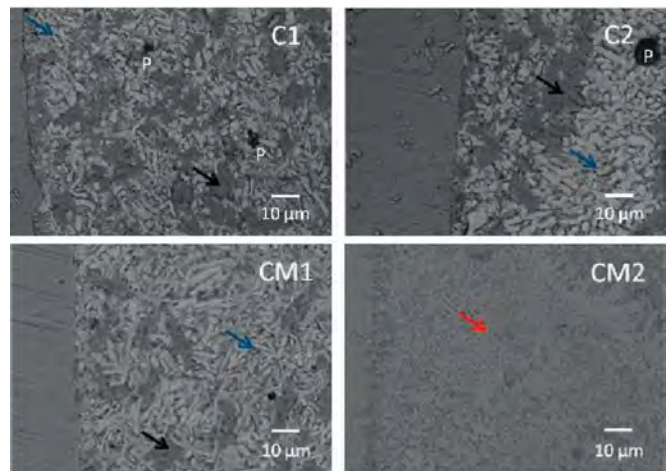


Fig. 3 Micrographs of steel–glass interfaces after an ageing operation of 1,000 h at 700 °C under air (black arrows: BaCa silicates, blue arrows: Ba silicates, red arrow: Mg silicates, p: pore).

Table 5 Results of hydrogen-tightness tests on steel–glass–steel assemblies at ambient temperature after an ageing operation of 1,000 h at 800 °C under air atmosphere (in vol.% of the measured flux on zirconia reference).

Samples	H ₂ out <i>t</i> = 0 h (vol.%)	H ₂ out <i>t</i> = 1,000 h (vol.%)	Comments
C1	100	30.5	Permeable
C2	100	11.5	Permeable
CM1	100	95.3	Few leaks
CM2	100	99.8	Gas-tight

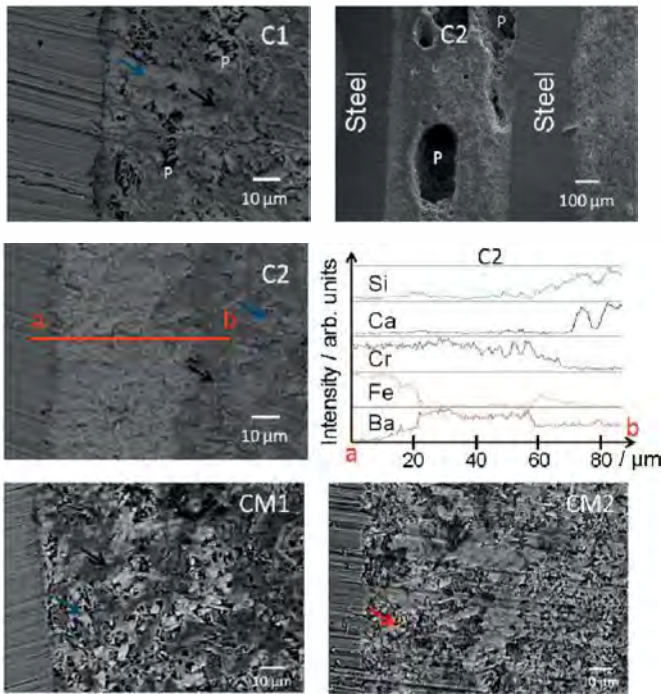


Fig. 4 Micrographs of steel–glass interfaces after an ageing operation of 1,000 h at 800 °C under air (black arrows BaCa silicates, blue arrows: Ba silicates, red arrow: Mg silicates, p: pore).

was detected at the C2 glass–steel interface. The EDX profile shows that the phase contains barium and chromium. In addition, pores of more than 100 μm in diameter were present in the C2 glass (Figure 4), which explained the permeability of this assembly. Big pores of about of 50 μm in diameter were also present in the C1 glass. Smaller pores were observed in the CM1 and CM2 glasses. Crystals in these glasses were less easily observable than after the ageing treatment at 700 °C. However, EDX analysis showed that there were still areas composed of barium–calcium silicates (gray) and barium silicates (white) crystals in the C1, C2, and CM1 glasses. The obtained microstructure of CM1 (acicular crystals) and CM2 (smaller crystals) materials were similar after an ageing operation in air for 1,000 h at 700 °C or at 800 °C. Considering the hydrogen-tightness obtained on the different seals, CM2 glass was chosen for the next step of this study.

3.3 Ageing Test of 1,000 h at 700 °C on an Assembly without Binder

A last assembly was realized with water as the binder of the glass paste in order to prove that the

amount of organic compounds could be reduced. First, the glass powder CM2 was ground to reduce the grain size ($D_{50} \sim 6 \mu\text{m}$). Then, this powder was mixed with water to form an aqueous slurry. This mixture has a lower viscosity than the glass paste formed with ethylcellulose/terpineol. As a result, when it was applied on a square steel (5 cm²), it was spread over a larger surface area and thickness of the joint has been reduced. Another square steel with a center hole of 10 mm was deposited after drying the paste to form a steel–glass–steel assembly. A sealing operation of 850 °C for 2 h was performed under the same conditions as for the previous steel–glass–steel assemblies. An ageing treatment in air at 700 °C identical to Section 3.1 was operated.

Intermediate and final hydrogen-tightness results obtained are presented in Table 6. The assembly made with glass paste “CM2 + water” was gas-tight (relative deviations from zirconia reference at the device output was inferior to 2%) throughout the thermal operations, demonstrating that the use of an aqueous route has no influence on the tightness of the seal. Considering this promising result, CM2 glass chemical composition was deposited onto two SOF cells using only water to make a glass paste. Electrical tests on these cells are described in the next part.

3.4 Characterization of Complete Fuel Cells with CM2 Glass as Sealant

The evolution of the OCV of the cells is reported in Figure 5. The OCV increased when the H₂ partial flux was gradually increased from 0 to 2 L.h⁻¹. After a small plateau due to the

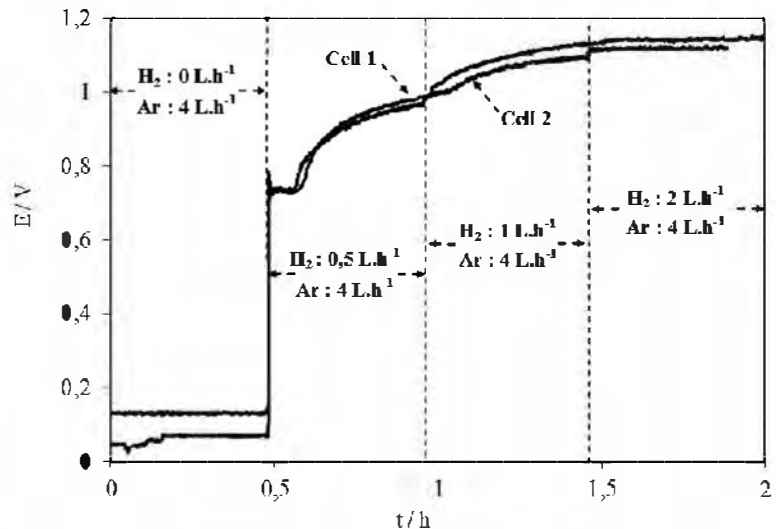


Fig. 5 Open circuit voltage measured on the cells sealed with CM2 glass during the reduction treatment.

Table 6 Results of hydrogen-tightness tests on a steel–glass CM2 without binder–steel assembly at ambient temperature after different ageing operations at 700 °C (until 1,000 h) under air atmosphere (in vol.% of the measured flux on zirconia reference).

Samples	$t = 0 \text{ h}$ H ₂ out (vol.%)	$t = 250 \text{ h}$ H ₂ out (vol.%)	$t = 500 \text{ h}$ H ₂ out (vol.%)	$t = 1000 \text{ h}$ H ₂ out (vol.%)	Comments
CM2 + water	100	99.5	100	101.1	Gas-tight

NiO/Ni equilibrium, the OCV stabilized around 1.11–1.12 V. This value is close to the theoretical 1.13 V obtained using the Nernst equation at this temperature. This observation indicated a good tightness of the sealant between the electrode compartments.

The electrochemical performances of the cells were determined at high temperature using hydrogen as the fuel with a flux of 2 L h^{-1} . Cell 1 was maintained at 800°C and cell 2 at 760°C in order to evaluate the tightness of the system at two different temperatures under load conditions, i.e., with the strong exothermicity of H_2 electrochemical oxidation, and its evolution as a function of time. The polarisation and power density curves obtained at steady state are given in Figure 6.

The values obtained were close to 180 mW cm^{-2} at 800°C (at 1.1 V) and 90 mW cm^{-2} at 760°C (at 0.6 V). The fuel cells used to evaluate the applicability of the glasses investigated in this study, were not fully optimized. The origin of the relatively low power density is not related to the glass sealing properties, and the promising stability demonstrated is independent from the cell performance.

As indicated in Figure 6, after a potentiostatic test of 2 h at 0.5 V, the power density of both cells was unchanged, indicating a good stability of the complete system under load conditions, and then a good gas-tightness ensured by the glass. Furthermore, the OCV of the cell 1 during the potentiostatic test at high temperature (Figure 7) was unchanged. Nonetheless, the OCV of the cell 2 was reduced by nearly 15% from the initial measure after 2 h (measures on cell 2 were stopped after every hour). After a mid-term operation on cell 1 ($\sim 2,000 \text{ h}$ at 800°C), careful SEM and EDX observations of the cathodic side of the fuel cell indicated that CM2 glass did not spread on the cells components during experiments at high temperature. These results were reported elsewhere [24].

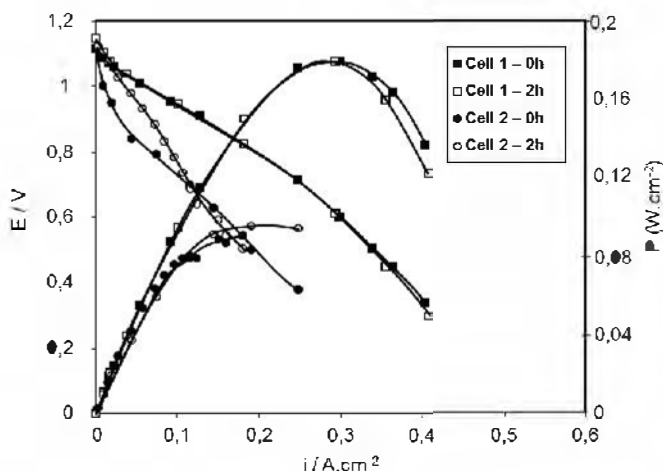


Fig. 6 Polarization curves of the cells sealed with CM2 glass at 800°C for cell 1 and at 760°C for cell 2.

4 Discussion

After a mid-term test of 1,000 h at 700°C , smaller crystals in CM2 were attributed to the formation of MgSiO_3 phase as already observed [19]. Microstructures of the four glasses after 1,000 h at 700 or 800°C are similar to that of glasses after an ageing operation of 100 h at 800°C [19]. Chemical compositions and amounts of crystalline phases are unchanged with a longer ageing time at high temperature. Consequently, structure and microstructure of the four glasses remain stable over long periods at high temperatures in air.

A barium chromate phase crystallized at the steel–C2 glass interface during the 1,000 h ageing operation at 800°C . BaCrO_4 has been described as a common product of a chemical reaction between the barium contained in the glass and the chromium present at the steel surface [14, 15]. This phase induces thermomechanical stresses that yields cracks between the glass and the surrounding materials during thermal cycles. Many authors had described different chemical interactions between glass seals and stainless steels (CROFER22APU...), which could lead to internal corrosion of the steel or to the formation of iron oxide nodules [16–18]. K41X is a ferritic steel with a chemical composition close to the CROFER22APU steel and various chemical reactions could happen at the metal–glass interface. However, the role of PbO in glass seals had been determined to be detrimental in these chemical reactions [16, 17]. Taking into account that PbO is not present in the selected glasses of this study, no undesirable reactions happened during mid-term tests. Furthermore, the high amount of BaO in glass seals could explain the absence of Fe-O phases at the metal–glass interface [18]. In order to complete these promising results, other experiments in dual atmosphere will be realized to observe possible chemical reactions at the interface between glasses and steel K41X.

The important porosity and pore size ($\geq 50 \mu\text{m}$) observed in C1 and C2 glasses after ageing at 800°C for 1,000 h caused the permeability of the assemblies using these materials as sea-

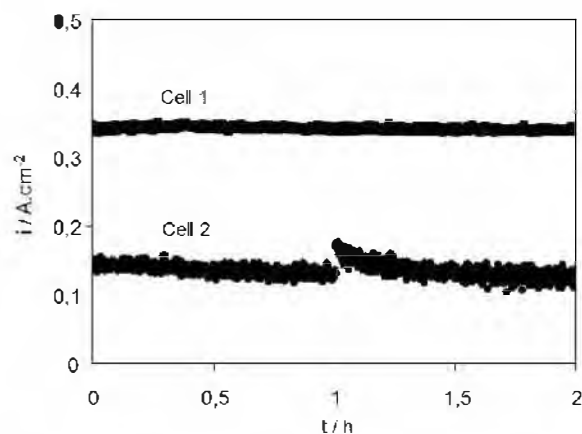


Fig. 7 Evolution of the current density of cells 1 and 2 at $E=0.5 \text{ V}$ as a function of time. Sealing was performed at 850°C during 2 h with argon (4 L h^{-1}) in the anodic compartment. Dry hydrogen was introduced gradually until 2 L h^{-1} at 800°C to reduce the anode.

lants. Nonetheless, the densification of all glasses was achieved before crystallization during the sealing operation of the assemblies. This observation is supported by the hydrogen-tightness of the assemblies after sealing. Consequently, pores were formed during the ageing treatment at 800 °C. Substitution of 5% CaO by 5% MgO between C2 and CM1 improved the gas-tightness, as well as 5% MgO addition in the CM2 glass. MgO plays a role in the obtention of gas-tight sealant. It was observed that barium–calcium silicate crystals were present in the C1, C2, and CM1 glasses after 100 h at 800 °C in air [21]. Only MgSiO₃ crystals were identified in CM2 glass in this case.

The following hypotheses can be proposed to understand the role of MgO in CM2 glass:

Crystallization activation energy is lower in BCAS glass than in magnesium alumino-borosilicate (BMAS) glass [2, 5]. In CM2 glass (containing 10 mol.% of MgO), a strong nucleation of MgSiO₃ occurred during sealing operation at 850 °C, giving little MgSiO₃ crystals. In other glasses, the sealing operation promote nucleation and growth of barium silicate and barium calcium silicate phases. Furthermore, we showed that CM2 glass had the highest half-ball temperature of the four material compared [19]. Crystallization of magnesium silicate crystals increases the viscosity of this glass more than the crystallization of the other compounds in the three other materials. Mechanical properties are better in this glass because of its special fine microstructure.

At lower temperature during ageing (700 or 800 °C), growth of all crystals is significantly reduced. CM2 glass is not modified over long term operation under air atmosphere.

Ionic radius of Mg²⁺ (0.066 nm) is smaller than ionic radius of Ca²⁺ (0.099 nm). Consequently, diffusion of Mg²⁺ is favored in glass containing MgO during the sealing operation. MgSiO₃ crystals are easily formed and silicon amount in residual glass is too low to promote the formation of other phases during ageing at lower temperature.

CM2 glass was considered as the most promising glass to seal an SOFC mainly because of weak hydrogen leaks. Microstructural observations confirmed that only few pores are present in the glass after 1,000 h at high temperature. As a consequence, porosity is supposed to be closed. Growth of pores or coalescence phenomenon are not favored because of the special microstructure of this material. Indeed, fine crystals allowed to obtain a mechanical stable glass–ceramic after the sealing operation. The amount of crystalline phases is supposed to be nearly the same after the sealing operation and after long ageing treatment because microstructure of glass does not evolve [19]. Chemical composition of crystals after a long treatment at high temperature need to be checked. Nonetheless, as the microstructure was not modified and the diffusion processes are limited, these chemical compositions are supposed to be quite similar.

The use of CM2 glass in complete fuel cells and the characterization of the systems confirmed that CM2 glass was adequate for SOFC applications at 800 °C. Indeed, the OCV of the cell 1 at 800 °C after few weeks at high temperature was

unchanged [24]. The decrease of the operating temperature at 760 °C reduces the power density of the cell by a factor 2. This decrease is due to losses of ionic conduction in the YSZ electrolyte and to the increase of all electrode overpotentials at lower temperatures.

Glass pastes could be made without binder to avoid porosity created by the degradation of organic compounds. However, if the hydrogen-tightness was not modified using an aqueous route, the application of the paste on SOFC components could be more difficult. So, the use of this kind of joint will depend on the design of the future SRU.

Other experiments on steel–glass–steel assemblies had been performed in H₂/H₂O atmosphere in order to observe degradation mechanisms of sealants under reducing conditions [19].

5 Conclusion

Mid-term tests at 800 °C during 1,000 h showed that only CM2 glass was suitable for SOFC operation because of the gas-tightness obtained using this material. Chemical interactions between the C2 glass with the higher CaO content and the K41X steel lead to the formation of the critical phase BaCrO₄. High porosity was observed in this glass as well as in the C1 glass. As a consequence, these pores yield hydrogen leakage. Some hypotheses on the role of MgO in CM1 and CM2 glasses were discussed. CM2 glass has a different microstructure as compared to the other sealant. Fine crystals attributed to MgSiO₃ phase stabilize the mechanical properties and avoid pores growth or coalescence phenomenon. Diffusion process could be reduced, which could prevent chemical reactions with steel.

The test of application of the paste without binder (only water) showed that CM2 glass could be applied in different ways without any difference in gas-tightness properties. The different uses of glass paste will depend on the design of future SRU.

Stable OCV values and cell performances at the initial step when using CM2 as a sealant confirmed the interest to use this material in SOFC application.

Acknowledgements

The authors wish to thank ADEME, GDF SUEZ, and EIFER for their financial support.

References

- [1] P. Stevens, F. Novel-Cattin, A. Hammou, C. Lamy, M. Cassir, *p. 1, Techn. de l'Ing.* **2000**, D3340, 0000.
- [2] J. W. Fergus, *J. Power Sources* **2005**, *147*, 46.
- [3] M. K. Mahapatra, K. Lu, *J. Power Sources* **2010**, *195*, 7129.
- [4] M. K. Mahapatra, K. Lu, *vol. 67, Mater. Sci. Eng.* **2010**, *67*, 65.
- [5] N. P. Bansal, E. A. Gamble, *J. Power Sources* **2005**, *147*, 107.

- [6] A. Flugel, M. D. Dolan, A. K. Varshneya, N. Colema, M. Hall, D. Earl, S. T. Misture, *J. Electrochem. Soc.* **2007**, *154*, 601B.
- [7] M. D. Dolan, S. T. Misture, *J. Electrochem. Soc.* **2007**, *154*, 700B.
- [8] C. Lara, M. J. Pascual, M. O. Prado, A. Duran, *Solid State Ion.* **2004**, *170*, 201.
- [9] T. Sun, H. Xiao, W. Guo, X. Hong, *Ceram. Int.* **2010**, *36*, 821.
- [10] S. B. Sohn, S. Y. Choi, G. H. Kim, H. S. Song, G. D. Kim, *J. Non-Cryst. Solids* **2002**, *297*, 103.
- [11] K. D. Meinhardt, D. S. Kim, Y. S. Chou, K. S. Weil, *J. Power Sources* **2008**, *182*, 188.
- [12] A. Goel, D. U. Tulyaganov, V. V. Kharton, A. A. Yaremchenko, S. Eriksson, J. M. F. Ferreira, *J. Power Sources* **2009**, *189*, 1032.
- [13] S. Ghosh, A. D. Sharma, A. K. Mukhopadhyay, P. Kundu, R. N. Basu, *Int. J. Hydrogen Energy* **2010**, *35*, 272.
- [14] Z. Yang, J. W. Stevenson, K. D. Meinhardt, *Solid State Ion.* **2003**, *160*, 213.
- [15] L. Peng, Q. Zhu, *J. Power Sources* **2009**, *194*, 880.
- [16] P. Batfalsky, V. A. C. Haanappel, J. Malzbender, N. H. Menzler, V. Shemet, I. C. Vinke, R. W. Steinbrech, *J. Power Sources* **2006**, *155*, 128.
- [17] V. A. C. Haanappel, V. Shemet, S. M. Gross, T. Koppitz, N. H. Menzler, M. Zahid, W. J. Quadackers, *J. Power Sources* **2005**, *150*, 86.
- [18] S. Gosh, A. D. Sharma, P. Kundu, S. Mahanty, R. N. Basu, *J. Non-Cryst. Solids* **2007**, *354*, 4081.
- [19] J. Puig, *Ph.D. Thesis*, Paul Sabatier University, Toulouse, France **2012**.
- [20] J. Puig, F. Ansart, P. Lenormand, L. Antoine, J. Dailly, *J. Non-Cryst. Solids* **2011**, *357*, 3490.
- [21] S. M. Gross, T. Koppitz, J. Rimmel, J.-B. Bouche, U. Reisinger, *Fuel Cells Bull.* **2006**, *vol. 2006*, 12.
- [22] J.-M. Klein, M. Hénault, Y. Bultel, P. Gélin, S. Georges, *Electrochem. Solid State Lett.* **2008**, *11*, 144B.
- [23] J.-M. Klein, M. Hénault, C. Roux, Y. Bultel, S. Georges, *J. Power Sources* **2009**, *193*, 331.
- [24] S. Georges, N. Bailly, M. C. Steil, Y. Bultel, A. Hadjar, J. P. Viricelle, M. Rieu, *ECS Trans.* **2013**, *57*, 3023. DOI: 10.1149/05701.3023ecst